BS ISO 14999-4:2015

BSI Standards Publication

Optics and photonics — Interferometric measurement of optical elements and optical systems

Part 4: Interpretation and evaluation of tolerances specified in ISO 10110

bsi.

...making excellence a habit.™

National foreword

This British Standard is the UK implementation of ISO 14999-4:2015. It supersedes BS ISO 14999-4:2007 which is withdrawn.

The UK participation in its preparation was entrusted to Technical Committee CPW/172, Optics and Photonics.

A list of organizations represented on this committee can be obtained on request to its secretary.

This publication does not purport to include all the necessary provisions of a contract. Users are responsible for its correct application.

ISBN 978 0 580 79515 2

ICS 37.020

Compliance with a British Standard cannot confer immunity from legal obligations.

This British Standard was published under the authority of the Standards Policy and Strategy Committee on 31 July 2015.

Amendments issued since publication

Date	Text affected

BS ISO 14999-4:2015

INTERNATIONAL STANDARD

ISO 14999-4

Second edition
2015-08-01

Optics and photonics — Interferometric measurement of optical elements and optical systems —

Part 4:
Interpretation and evaluation of tolerances specified in ISO 10110

Optique et photonique — Mesurage interférométrique de composants et de systèmes optiques —

Partie 4: Directives pour l'évaluation des tolérances spécifiées dans l'ISO 10110

Reference number
ISO 14999-4:2015(E)

Contents

Page

Foreword

ISO (the International Organization for Standardization) is a worldwide federation of national standards bodies (ISO member bodies). The work of preparing International Standards is normally carried out through ISO technical committees. Each member body interested in a subject for which a technical committee has been established has the right to be represented on that committee. International organizations, governmental and non-governmental, in liaison with ISO, also take part in the work. ISO collaborates closely with the International Electrotechnical Commission (IEC) on all matters of electrotechnical standardization.

The procedures used to develop this document and those intended for its further maintenance are described in the ISO/IEC Directives, Part 1. In particular the different approval criteria needed for the different types of ISO documents should be noted. This document was drafted in accordance with the editorial rules of the ISO/IEC Directives, Part 2 (see www.iso.org/directives).

Attention is drawn to the possibility that some of the elements of this document may be the subject of patent rights. ISO shall not be held responsible for identifying any or all such patent rights. Details of any patent rights identified during the development of the document will be in the Introduction and/or on the ISO list of patent declarations received (see www.iso.org/patents).

Any trade name used in this document is information given for the convenience of users and does not constitute an endorsement.

For an explanation on the meaning of ISO specific terms and expressions related to conformity assessment, as well as information about ISO's adherence to the WTO principles in the Technical Barriers to Trade (TBT) see the following URL: Foreword - Supplementary information.

The committee responsible for this document is ISO/TC 172, *Optics and photonics*, Subcommittee SC 1, *Fundamental standards*.

This second edition cancels and replaces the first edition (ISO 14999-4:2007), which constitutes the following changes:

a) clauses for tolerancing cylindrical and torical wavefronts, the representation of the measured wavefront deformation in terms of Zernike coefficients, and for tolerancing of the slope deviation have been added;

b) the name of quantity A has been changed to power deviation. For further details, see 3.3.1, Note 2 to entry.

ISO 14999 consists of the following parts, under the general title *Optics and photonics — Interferometric measurement of optical elements and optical systems*:

— *Part 1: Terms, definitions and fundamental relationships* [Technical Report]

— *Part 2: Measurement and evaluation techniques* [Technical Report]

— *Part 3: Calibration and validation of interferometric test equipment and measurements* [Technical Report]

— *Part 4: Interpretation and evaluation of tolerances specified in ISO 10110*

Introduction

This part of ISO 14999 provides a theoretical frame upon which are based indications from ISO 10110-5 and/or ISO 10110-14.

A table listing the corresponding nomenclature, functions, and values used in ISO 10110-5 and ISO 14999-4 is given in ISO 10110-5, Annex B.

ISO 10110-5 refers to deformations in the form of an optical surface and provides a means for specifying tolerances for certain types of surface deformations in terms of “nanometers”.

ISO 10110-14 refers to deformations of a wavefront transmitted once through an optical system and provides a means of specifying similar deformation types in terms of optical “wavelengths”.

As it is common practice to measure the surface form deviation interferometrically as the wavefront deformation caused by a single reflection from the optical surface at normal (90° to surface) incidence, it is possible to describe a single definition of interferometric data reduction that can be used in both cases. One “fringe spacing” (as defined in ISO 10110-5) is equal to a surface deformation that causes a deformation of the reflected wavefront of one wavelength.

Certain scaling factors apply depending on the type of interferometric arrangement, e.g. whether the test object is being measured in single pass or double pass.

Due to the potential for confusion and misinterpretation, units of nanometres rather than units of “fringe spacings” or “wavelengths” are to be used for the value of surface form deviation or the value of wavefront deformation, where possible. Where “fringe spacings” or “wavelengths” are used as units, the wavelength is also to be specified.

Optics and photonics — Interferometric measurement of optical elements and optical systems —

Part 4: Interpretation and evaluation of tolerances specified in ISO 10110

1 Scope

This part of ISO 14999 applies to the interpretation of interferometric data relating to the measurement of optical elements.

This part of ISO 14999 gives definitions of the optical functions and values specified in the preparation of drawings for optical elements and systems, made in accordance with ISO 10110-5 and/or ISO 10110-14 for which the corresponding nomenclature, functions, and values are listed in ISO 10110-5, Annex B. It also provides guidance for their interferometric evaluation by visual analysis.

2 Normative references

The following documents, in whole or in part, are normatively referenced in this document and are indispensable for its application. For dated references, only the edition cited applies. For undated references, the latest edition of the referenced document (including any amendments) applies.

ISO 10110-5, *Optics and photonics — Preparation of drawings for optical elements and systems — Part 5: Surface form tolerances*

ISO 10110-14, *Optics and photonics — Preparation of drawings for optical elements and systems — Part 14: Wavefront deformation tolerance*

ISO/TR 14999-2, *Optics and photonics — Interferometric measurement of optical elements and optical systems — Part 2: Measurement and evaluation techniques*

3 Terms and definitions

3.1 Mathematical definitions

3.1.1
function
mathematical description of the measured wavefront deformation and its decomposition into components

Note 1 to entry: The functions used in this part of ISO 14999 are scalar functions.

3.1.2
peak-to-valley value
PV (f)
<of a function f> maximum value of the function within the region of interest minus the minimum value of the function within the region of interest

3.1.3
root mean square value
rms (f)
<of a function f over a given area A> value given by either of the following integral expressions:

a) Cartesian variables x and y

$$\text{rms}\,(f)=\left[\frac{\int\limits_{x}\int\limits_{y}\left[f\left(x,y\right)\right]^{2}\,\mathrm{d}x\,\mathrm{d}y}{\int\limits_{x}\int\limits_{y}\mathrm{d}x\,\mathrm{d}y}\right]^{1/2}\quad \text{where } \left(x,y\right)\in A$$

b) Polar variables r and θ

$$\text{rms}\,(f)=\left[\frac{\int\limits_{\theta}\int\limits_{r}\left[f\left(r,\theta\right)\right]^{2}\,r\,\mathrm{d}r\,\mathrm{d}\theta}{\int\limits_{\theta}\int\limits_{r}r\,\mathrm{d}r\,\mathrm{d}\theta}\right]^{1/2}\quad \text{where } \left(r,\theta\right)\in A$$

Note 1 to entry: This integral may be approximated by the standard deviation if the usage includes removal of the mean value of the wavefront (piston) and provided that the measurement resolution is specified and is sufficient.

3.2 Definition of optical functions

NOTE 1 For the relationship of interferometric measurements to surface form deviation and transmitted wavefront deformation, see Clause 4.

NOTE 2 The optical functions given in this subclause are used either for rotationally invariant (spherical or aspherical) wavefronts (depicted in Figure 1) or cylindrical wavefronts (depicted in Figure 2). The functions corresponding to each are grouped together; the functions for rotationally invariant wavefronts first and the functions for cylindrical wavefronts follow. The functions for rotationally invariant wavefronts are unchanged with respect to ISO 14999-4:2007.

NOTE 3 The term cylindrical waveform is used here as synonym for circular cylindrical, non-circular cylindrical, and torical wavefronts. The functions can also be applied for general wavefronts that are close to cylindrical or torical ones.

3.2.1
measured wavefront deformation

f_{MWD}

function representing the distances between the measured wavefront and the nominal theoretical wavefront, measured normal to the nominal theoretical wavefront

Note 1 to entry: See Figure 1 a) and Figure 2 a).

Note 2 to entry: In case of tactile measurement where the measurement values are usually taken along z-direction, the measurement values have to be converted to the measured wavefront deformation f_{MWD} (distance perpendicular to the theoretical surface).

3.2.2
tilt

f_{TLT}

plane function representing the best (in the sense of the rms fit) linear approximation to the measured wavefront deformation f_{MWD}

Note 1 to entry: See Figure 1 b) and Figure 2 b).

3.2.3
twist-function describing rotational misalignment for cylindrical wavefronts

f_{TWST}

function of the saddle form used for eliminating rotational misalignment

$$f_{\mathrm{TWST}}(x,y)=const.*x*y$$

Note 1 to entry: See Figure 2 c).

Note 2 to entry: A rotational misalignment (twist) of the cylindrical axes of the test wave and the surface (respectively, the object under test and the optics generating or compensating the cylindrical or torical phase front) results in an additive term in the form of a saddle. This term could be eliminated or minimized by careful alignment of the setup. In most practical cases, it is more useful to eliminate this term by removing it mathematically.

3.2.4
wavefront deformation
f_{WD}
function resulting after subtraction of the tilt f_{TLT} from the measured wavefront deformation f_{MWD}

$$f_{\text{WD}} = f_{\text{MWD}} - f_{\text{TLT}}$$

Note 1 to entry: See Figure 1 c).

3.2.5
wavefront deformation for cylindrical wavefronts
$f_{\text{WD,CY}}$
function resulting after subtraction of the tilt f_{TLT} and f_{TWST} from the measured wavefront deformation, f_{MWD}

$$f_{\text{WD,CY}}(x,y) = f_{\text{MWD}}(x,y) - f_{\text{TLT}}(x,y) - f_{\text{TWST}}(x,y)$$

Note 1 to entry: See Figure 2 d).

3.2.6
wavefront spherical approximation
f_{WS}
function of spherical form that best (in the sense of the rms fit) approximates the wavefront deformation f_{WD}

Note 1 to entry: See Figure 1 d).

3.2.7
wavefront circular cylindrical approximation
$f_{\text{WC, x}}$, $f_{\text{WC, y}}$
functions of cylindrical form that best (in the sense of the rms fit) approximate the wavefront deformation $f_{\text{WD,CY}}$

$$f_{\text{WC,x}}(x,y) = R_{\text{x,fit}} - \sqrt{R_{\text{x,fit}}{}^2 - x^2} + const.$$

$$f_{\text{WC,y}}(x,y) = R_{\text{y,fit}} - \sqrt{R_{\text{y,fit}}{}^2 - y^2} + const.$$

Note 1 to entry: See Figure 2 e) and Figure 2 f).

3.2.8
wavefront irregularity
f_{WI}
function resulting after subtraction of the wavefront spherical approximation f_{WS} from the wavefront deformation f_{WD}

$$f_{\text{WI}} = f_{\text{WD}} - f_{\text{WS}}$$

Note 1 to entry: See Figure 1 e).

3.2.9
wavefront irregularity for cylindrical wavefronts
$f_{\mathrm{WI, CY}}$
function resulting after subtraction of the wavefront circular cylindrical approximations $f_{\mathrm{WC, x}}$ and $f_{\mathrm{WC, y}}$

$$f_{\mathrm{WI, CY}}(x, y) = f_{\mathrm{WD, CY}}(x, y) - f_{\mathrm{WC,x}}(x, y) - f_{\mathrm{WC,y}}(x, y)$$

Note 1 to entry: See Figure 2 g).

3.2.10
wavefront aspheric approximation
f_{WRI}
rotationally invariant aspherical function that best (in the sense of the rms fit) approximates the wavefront irregularity, f_{WI}

Note 1 to entry: See Figure 1 f).

3.2.11
wavefront non-circular cylindrical approximation
$f_{\mathrm{WTI, x}}$, $f_{\mathrm{WTI, y}}$
translationally invariant non-circular cylindrical function that best (in the sense of the rms fit) approximates the wavefront irregularity for cylindrical wavefronts, $f_{\mathrm{WI, CY}}$ in x and y direction, respectively

$$f_{\mathrm{WTI,x}}(x, y) = f_{\mathrm{WTI,x}}(x)$$

$$f_{\mathrm{WTI,y}}(x, y) = f_{\mathrm{WTI,y}}(y)$$

Note 1 to entry: See Figure 2 h) and Figure 2 i).

3.2.12
rotationally varying wavefront deviation
f_{WRV}
function resulting after subtraction of the wavefront aspheric approximation f_{WRI} from the wavefront irregularity f_{WI}

$$f_{\mathrm{WRV}} = f_{\mathrm{WI}} - f_{\mathrm{WRI}}$$

Note 1 to entry: See Figure 1 g).

3.2.13
translationally varying wavefront deviation
f_{WTV}
function resulting after subtraction of the wavefront non-circular cylindrical approximation $f_{\mathrm{WTI, x}}$ and $f_{\mathrm{WTI, y}}$

$$f_{\mathrm{WTV}} = f_{\mathrm{WI,CY}} - f_{\mathrm{WTI,x}} - f_{\mathrm{WTI,y}}$$

Note 1 to entry: See Figure 2 j).

3.3 Definition of values related to the optical functions defined in 3.2

3.3.1
power deviation
PV (f_{WS})
peak-to-valley value of the approximating spherical wavefront

Note 1 to entry: PV (f_{WS}) corresponds to the quantity A in ISO 10110-5 and ISO 10110-14.

Note 2 to entry: Previous versions of this part of ISO 14999 used the term sagitta deviation to represent this value. For better clarity, the term sagitta deviation has been replaced with power deviation to more accurately reflect the distance normal to a reference surface, whereas sagitta deviation refers to the distance parallel to the *z* axis to the surface.

3.3.2
power deviation for cylindrical wavefronts
PV ($f_{\mathrm{WC,\,x}}$), PV ($f_{\mathrm{WC,\,y}}$)
peak-to-valley value of the approximating circular cylindrical wavefronts in *x* and *y* direction, respectively

Note 1 to entry: PV ($f_{\mathrm{WC,\,x}}$) corresponds to the quantity AX and PV ($f_{\mathrm{WC,\,y}}$) to the quantity AY in ISO 10110-5 and ISO 10110-14.

3.3.3
irregularity
PV (f_{WI})
peak-to-valley value of the wavefront irregularity

Note 1 to entry: PV (f_{WI}) corresponds to the quantity B in ISO 10110-5 and ISO 10110-14.

3.3.4
irregularity for cylindrical wavefronts
PV ($f_{\mathrm{WI,\,CY}}$)
peak-to-valley value of the wavefront irregularity for cylindrical wavefronts

Note 1 to entry: PV ($f_{\mathrm{WI,\,CY}}$) corresponds to the quantity B in ISO 10110-5 and ISO 10110-14.

3.3.5
rotationally invariant irregularity
PV (f_{WRI})
peak-to-valley value of the wavefront aspheric approximation

Note 1 to entry: PV (f_{WRI}) corresponds to the quantity C in ISO 10110-5 and ISO 10110-14.

3.3.6
translationally invariant irregularity for cylindrical wavefronts
PV ($f_{\mathrm{WTI,\,x}}$), PV ($f_{\mathrm{WTI,\,y}}$)
peak-to-valley value of the wavefront non-circular cylindrical approximation

Note 1 to entry: PV ($f_{\mathrm{WTI,\,x}}$) corresponds to the quantity CX and PV ($f_{\mathrm{WTI,\,y}}$) to the quantity CY in ISO 10110-5 and ISO 10110-14.

3.3.7
rotationally varying irregularity
PV (f_{WRV})
peak-to-valley value of the remaining rotationally varying wavefront deviation

3.3.8
translationally varying irregularity
PV(f_{WTV})
peak-to-valley value of the remaining translational varying wavefront deviation

3.3.9
rms total
rms (f_{WD})
root-mean-square value of the wavefront deformation

Note 1 to entry: rms (f_{WD}) corresponds to the quantity RMSt in ISO 10110-5 and ISO 10110-14.

3.3.10
rms total for cylindrical wavefronts
rms ($f_{WD, CY}$)
root-mean-square value of the wavefront deformation for cylindrical wavefronts

Note 1 to entry: rms ($f_{WD, CY}$) corresponds to the quantity RMSt in ISO 10110-5 and ISO 10110-14.

3.3.11
rms irregularity
rms (f_{WI})
root-mean-square value of the wavefront irregularity

Note 1 to entry: rms (f_{WI}) corresponds to the quantity RMSi in ISO 10110-5 and ISO 10110-14.

3.3.12
rms irregularity for cylindrical wavefronts
rms ($f_{WI, CY}$)
root-mean-square value of the wavefront irregularity for cylindrical wavefronts

Note 1 to entry: rms ($f_{WI, CY}$) corresponds to the quantity RMSi in ISO 10110-5 and ISO 10110-14.

3.3.13
rms rotationally invariant irregularity
rms (f_{WRI})
root-mean-square value of the wavefront aspheric approximation

3.3.14
rms translationally invariant irregularity
rms ($f_{WTI, x}$), rms ($f_{WTI, y}$)
root-mean-square value of the wavefront non-circular cylindrical approximation

3.3.15
rms rotationally varying irregularity
rms (f_{WRV})
root-mean-square value of the remaining rotationally varying wavefront deviation

Note 1 to entry: rms (f_{WRV}) corresponds to the quantity RMSa in ISO 10110-5 and ISO 10110-14.

3.3.16
rms translationally varying irregularity
rms (f_{WTV})
root-mean-square value of the remaining translational varying wavefront deviation

Note 1 to entry: rms (f_{WTV}) corresponds to the quantity RMSa in ISO 10110-5 and ISO 10110-14.

3.3.17
peak–to-valley deviation
PV (f_{WD})
peak-to-valley deviation of the wavefront deformation

Note 1 to entry: PV(f_{WD}) corresponds to the quantity of PV(Q) in ISO 10110-5 and ISO 10110-14.

3.3.18
peak-to-valley deviation for cylindrical wavefronts
PV($f_{WD,cy}$)
peak-to-valley deviation of the wavefront deformation for cylindrical wavefronts

Note 1 to entry: PV($f_{WD,cy}$) corresponds to the quantity of PV(Q) in ISO 10110-5 and ISO 10110-14.

3.3.19
robust peak–to-valley deviation
PVr (f_{WD})
robust estimate of the amplitude of a surface or wavefront measured using a digital interferometer and evaluated from the peak-to-valley value of a 36 term Zernike polynomial fit plus three times the root-mean-square value of the residual after removal of the Zernike polynomial fit[4]

Note 1 to entry: The terms Z(N≤10) and Z(12,0) from Annex B are being used for the 36 term fit.

Note 2 to entry: PVr(f_{WD}) corresponds to the quantity of PVr(R) in ISO 10110-5 and ISO 10110-14.

Note 3 to entry: This specification is not recommended for non-circular areas.

Note 4 to entry: The robust peak-to-valley deviation is a tolerance specification that has been recently defined[4] and is increasingly used for specifications.

3.4 Definition of Zernike polynomials

The Zernike polynomials and their referencing are given in Annex B, originating from ISO/TR 14999-2.

3.5 Definitions of functions and terms for tolerancing the slope deviation

3.5.1
function after detrending
f_{det}
function resulting after detrending the measured wavefront deformation f_{MWD}

Note 1 to entry: The tolerance of the slope deviation describes local surface form deviations. Therefore, a detrending of the function f_{MWD} before calculating the slope deviation can be useful. The type of detrending should be defined in the drawing. For instance, f_{det} can be calculated by removing the component described by the Zernike polynomial with the coefficients Z($N \le 8$) from f_{MWD} or by using the wavefront aspheric or non-circular cylindric approximation f_{WRI} or $f_{WTI,x}$, $f_{WTI,y}$ as f_{det}. The detrending shall be done prior to the calculation of the slope deviation. These procedures are in accordance to the considerations given in ISO 4287 and ISO 25178.

3.5.2
local slope deviation for one-dimensional measurements
$\xi_{1\text{-dim}}$
angular deviation of the local normal of the actual (real) surface from the normal of the theoretical surface, measured by means of a one-dimensional measurement with x denoting an arbitrary direction, as shown in the following formula:

$$\cos(\xi_{1-\text{dim}}) = \frac{1}{\sqrt{1+\left(\frac{df_{\text{det}}}{dx}\right)^2}}$$

3.5.3
local slope deviation for two-dimensional measurements
$\xi_{2\text{-dim}}$
angular deviation of the local normal of the actual (real) surface from the normal of the theoretical surface, measured by a two-dimensional measurement with x and y denoting arbitrary directions that are orthogonal to each other, as shown in the following formula:

$$\cos(\xi_{2-\text{dim}}) = \frac{1}{\sqrt{1+\left(\frac{\partial f_{\text{det}}}{\partial x}\right)^2+\left(\frac{\partial f_{\text{det}}}{\partial y}\right)^2}}$$

3.5.4
spatial sampling interval
distance between two neighbouring points, at which values of the function f_{det} are measured for the determination of the slope deviation

Note 1 to entry: The spatial sampling interval is specified by the quantities H and M in ISO 10110-5.

Note 2 to entry: Depending on the used measurement equipment, the distance of the measurement points can be slightly different from the specified spatial sampling interval. For calculating the slope deviation, the measured values shall be used.

3.5.5
sampling length
<one-dimensional slope measurement> distance for which the function f_{det} is fitted by a line to calculate the slope deviation at the centre point of the sampling length interval

Note 1 to entry: The sampling length is specified by the quantities G and L in ISO 10110-5 for one-dimensional measurements.

3.5.6
edge length of sampling area
<two-dimensional slope measurement> side length of the square for which the function f_{det} is fitted by a plane to calculate the slope deviation at the centre point of the sampling area

Note 1 to entry: The edge length of sampling area is specified by the quantities G and L in ISO 10110-5 for two-dimensional measurements.

3.6 Definitions of values for tolerancing the slope deviation

3.6.1
maximum value of the slope deviation (one-dimensional measurement)
$\max(\xi_{1\text{-dim}})$
maximum value of the slope deviation (for one-dimensional measurement)

Note 1 to entry: The maximum value of the slope deviation corresponds to the quantity F in ISO 10110-5.

3.6.2
maximum value of the slope deviation (two-dimensional measurement)
$\max(\xi_{2\text{-dim}})$
maximum value of the slope deviation (for two-dimensional measurement)

Note 1 to entry: The maximum value of the slope deviation corresponds to the quantity F in ISO 10110-5.

3.6.3
rms of the slope deviation (one-dimensional measurement)
$\text{rms}(\xi_{1\text{-dim}})$
root-mean-square value of the slope deviation (for one-dimensional measurement)

Note 1 to entry: The rms value of the slope deviation corresponds to the quantity K in ISO 10110-5.

3.6.4
rms of the slope deviation (two-dimensional measurement)
$\text{rms}(\xi_{2\text{-dim}})$
root-mean-square value of the slope deviation (for two-dimensional measurement)

Note 1 to entry: The rms value of the slope deviation corresponds to the quantity K in ISO 10110-5.

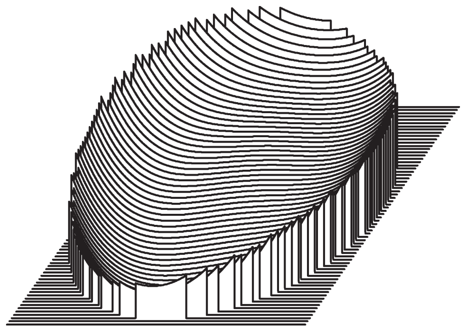

a) Measured wavefront deformation (f_{MWD})

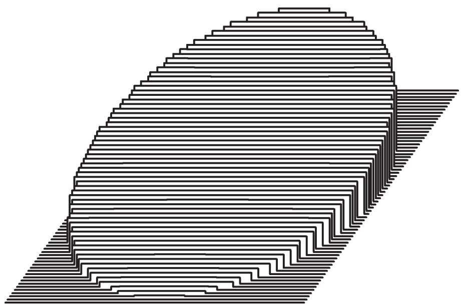

b) Tilt (f_{TLT})

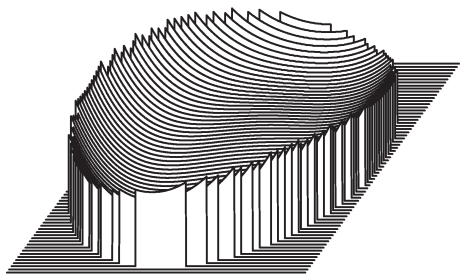

c) Wavefront deformation (f_{WD}) that determines the "RMSt"

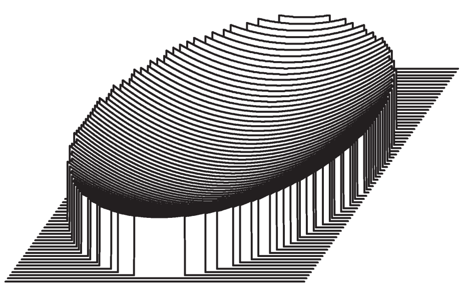

d) Wavefront spherical approximation (f_{WS}) that determines the power deviation "A"

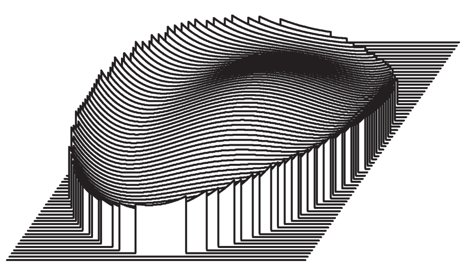

e) Wavefront irregularity (f_{WI}) that determines the irregularity "B" and "RMSi"

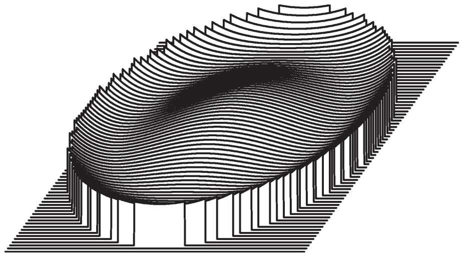

f) Rotationally invariant wavefront aspheric approximation (f_{WRI}) that determines the rotationally invariant irregularity "C"

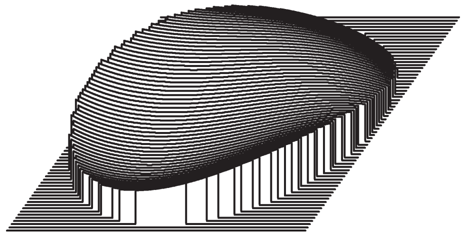

g) Remaining rotationally varying wavefront deviation (f_{WRV}) that determines the rotationally varying irregularity "RMSa"

Figure 1 — Measured wavefront deformation and its decomposition into wavefront deformation types

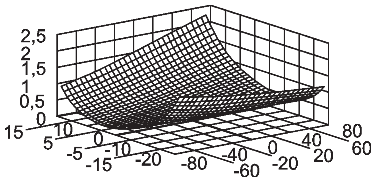

a) Measured wavefront deformation (f_{MWD})

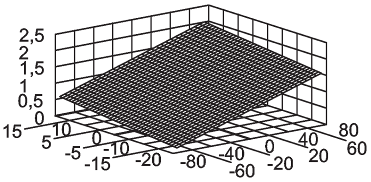

b) Tilt (f_{TLT})

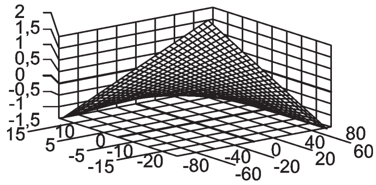

c) Function describing rotational misalignment f_{TWST}(x,y)

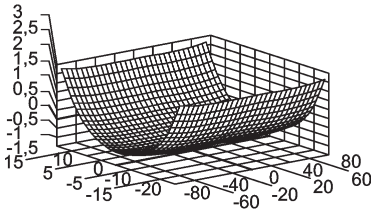

d) Wavefront deformation ($f_{\mathrm{WD,CY}}$) that determines “RMSt”

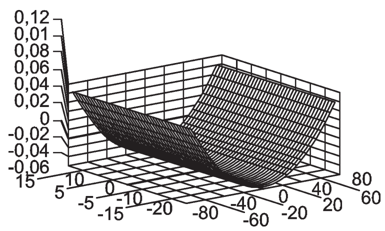

e) Wavefront circular-cylindrical approximation in x direction ($f_{\mathrm{WC,\ x}}$) that determines the power deviation “AX”

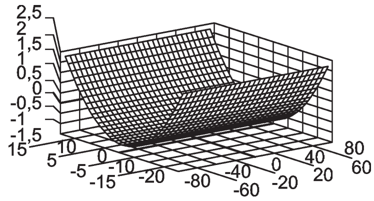

f) Wavefront circular-cylindrical approximation in y direction ($f_{\mathrm{WC,y}}$) that determines the power deviation “AY”

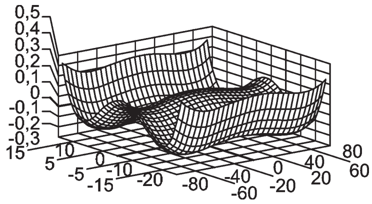

g) Wavefront irregularity ($f_{\mathrm{WI,\ CY}}$) that determines the irregularity “B” and “RMSi”

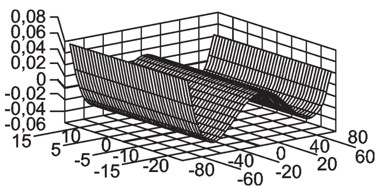

h) Translationally invariant wavefront non-circular cylindrical approximation in x direction ($f_{\mathrm{WTI,x}}$) that determines the translationally invariant irregularity “CX”

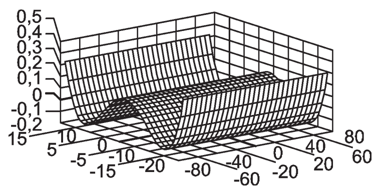

i) Translationally invariant wavefront non-circular cylindrical approximation in y direction ($f_{\mathrm{WTI,y}}$) that determines the translationally invariant irregularity “CY”

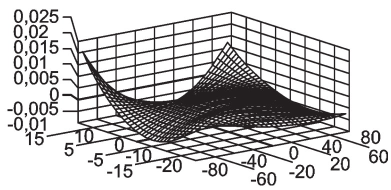

j) Remaining translationally varying wavefront deviation (f_{WTV}) that determines the translationally varying irregularity “RMSa”

Figure 2 — Measured wavefront deformation for cylindrical and torical wavefronts and its decomposition into wavefront deformation types

4 Relating interferometric measurements to surface form deviation or transmitted wavefront deformation

4.1 Test areas

The optical functions defined in 3.2 are only defined within the specified test areas.

NOTE If the test area is non-circular, the wavefront deformation decomposition cannot be made by Zernike polynomials.

4.2 Quantities

The quantities defined in 3.3 are used for the indications according to ISO 10110-5 and ISO 10110-14 using the specified fringe spacings or wavelength or nanometer as unit.

An optical path difference of one wavelength in the wavefront (one fringe spacing) corresponds to a surface form deviation of half a wavelength when reflected once at normal incidence.

4.3 Single-pass transmitted wavefront deformation

Transmitted wavefront deformation as defined in ISO 10110-14, is directly measurable using a single-pass arrangement, such as a Mach-Zehnder interferometer, provided that the wavelength of the interferometer is the same as the wavelength of the specification.

4.4 Double-pass transmitted wavefront deformation

Double-pass arrangements are often used to measure the transmitted wavefront deformation of optical elements by common path instruments. In this case, the interferometric measurement is approximately twice as sensitive. The interferometric results shall be divided by two to obtain approximate results for the transmitted wavefront deformation.

NOTE Since diffraction occurs at both passes through the test object and since the wavefront deformation imparted by the test object on the second pass depends slightly on the wavefront deformation imparted on the first pass, the transmitted wavefront deformation measured in a double-pass arrangement is only approximately half the results reported by the interferometer.

4.5 Surface form deviation

Surface form deviation is commonly measured using an interferometric measurement of a wavefront reflected once from the optical surface under test.

An optical path difference of one wavelength in the wavefront (one fringe spacing) corresponds to a surface form deviation of half a wavelength when reflected once at normal incidence.

4.6 Conversion to other wavelengths

If the test wavelength is not equal to the specification wavelength, the results of the interferometric test shall be converted using Formula (1):

$$N_{\lambda 2} = N_{\lambda 1} \times \frac{\lambda_1}{\lambda_2} \tag{1}$$

where

$N_{\lambda 1}$ and $N_{\lambda 2}$ are, for example, the numbers of fringe spacings at λ_1 and λ_2.

5 Representation of the measured wavefront deviation as Zernike coefficients

Optical components or systems can require a more detailed tolerance description than is possible by the values given in 3.3. It is common practice to apply coefficients of an orthogonal polynomial system to describe surfaces or wavefronts. A more detailed description of this approach is given in ISO/TR 14999-2. This part of ISO 14999 refers only to the Zernike coefficients for circular and elliptical areas.

The measured wavefront deformation f_{MWD} can be approximated by an analytic function yielding a global representation expressed by a number of Zernike coefficients (see ISO/TR 14999-2, 4.8). The Zernike polynomials and the nomenclature are given in Annex B. The coefficients may be given in addition to the values specified in 3.3.

For specifying the tolerance of the surface or wavefront, the tolerance band of individual coefficients or numeric combinations of the coefficients can be required. Also, the rms value and/or the peak-to-valley value of the approximation function described by a set of the Zernike polynomials can be required. Therefore, the wavefront deviation tolerance described by Zernike coefficients is defined as peak-to-valley PV(Z(n,m)) or PV(Z(N)) corresponding to Z(n,m) (PV < O) or Z(N) (PV < O) or as root-mean-square value Z(n,m) (RMS < P) or Z(N) (RMS < P) in ISO 10110-5.

NOTE 1 The unit of the coefficients is normally nm.

NOTE 2 Special care has to be taken not to mistake the coefficients describing the surface form or the wavefront with the coefficients describing the measurement deviation f_{MWD}.

EXAMPLES Examples are given in ISO 10110-5, 5.4.2.

6 Tolerancing of the slope deviation

Because local figuring with small tools is generally used for generating aspherical surfaces, an additional tolerance for the slope deviation, which limits the waviness of the surface, should be introduced.

The tolerance of the slope deviation describes local surface form deviations. Therefore, it might be useful to detrend the measurement data before calculating the slope deviation. This procedure should be defined in the drawing.

This part of ISO 14999 considers the distance between the measured surface and the theoretical surface. The distance is measured perpendicular to the theoretical surface; that is, along the theoretical surface normal. Therefore, for an ideal part where the measured wavefront is the same as the theoretical wavefront, the difference is zero for all points on the surface, which would define a plane $z = 0$, wherein the normal lies in z-direction for all points on the surface. Hence, the slope deviation can be expressed by means of the gradient.

For the slope deviation, rms–values and the maximum value of the slope deviation can be required. Slope deviation tolerance is defined as the maximum permissible value max($\xi_{\text{1-dim}}$) or max ($\xi_{\text{2-dim}}$) corresponding to the quantity ΔSv,w(F/G/H) in ISO 10110-5 or as the root-mean-square value rms($\xi_{\text{1-dim}}$) or rms($\xi_{\text{2-dim}}$) corresponding to the quantity RMS ΔSv,w(K/L/M) in ISO 10110-5.

According to ISO 10110-5, ISO 10110-12, and ISO 10110-14, different values of the slope deviation are allowed in different regions of the measurement area.

6.1 One-dimensional measurement of the slope deviation

When using this kind of tolerance definition, the slope of the surface is only evaluated by a line wise measurement, which is consistent with tactile measurements. Nevertheless, the slope deviation tolerance applies to the complete test area or the defined areas (see ISO 10110-5). Hence, no starting or reference points are given.

The measurement of the slope deviation can be required in one or several directions: arbitrary, x, y, radial ρ, or, tangential φ direction. See Figure 3.

For different directions of the measurement, different values of the slope deviation can be required (see ISO 10110-5, ISO 10110-12, and ISO 10110-14).

Table 1 gives the indications of the tolerance values for ISO 10110-5.

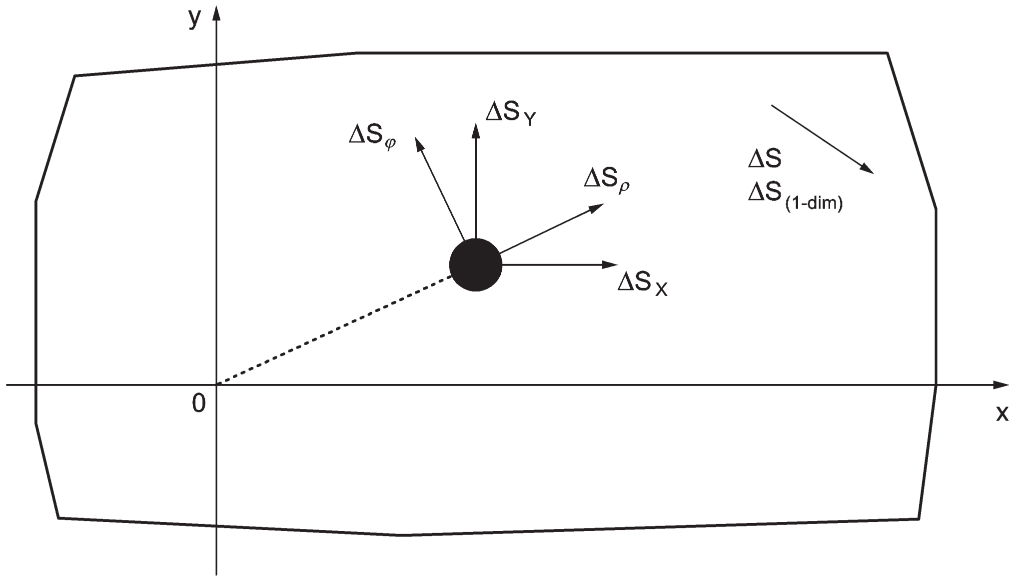

Figure 3 — Directions for line-wise measurement of the slope deviation

Table 1 — Indication of the tolerance values for one-dimensional measurements

Direction of measurement	Indication	Value	Indication	Value
Slope deviation in arbitrary direction	ΔS $\Delta S_{1\text{-dim}}$	$\max(\xi_{1\text{-dim}})$	$RMS\Delta S$ $RMS\Delta S_{1\text{-dim}}$	$\text{rms}(\xi_{1\text{-dim}})$
Slope deviation in x–direction	ΔS_X	$\max(\xi_{1\text{-dim}})$	$RMS\Delta S_X$	$\text{rms}(\xi_{1\text{-dim}})$
Slope deviation in y–direction	ΔS_Y	$\max(\xi_{1\text{-dim}})$	$RMS\Delta S_Y$	$\text{rms}(\xi_{1\text{-dim}})$
Slope deviation in radial direction	ΔS_ρ	$\max(\xi_{1\text{-dim}})$	$RMS\Delta S_\rho$	$\text{rms}(\xi_{1\text{-dim}})$
Slope deviation in tangential direction	ΔS_ϕ	$\max(\xi_{1\text{-dim}})$	$RMS\Delta S_\phi$	$\text{rms}(\xi_{1\text{-dim}})$

When using the one-dimensional measurement, the angle of the surface normal is only measured in the plane that contains the measurement direction and that is perpendicular to the x-y-plane. The slope deviation in the perpendicular direction is not included. So the slope deviation value can be lower than the real value.

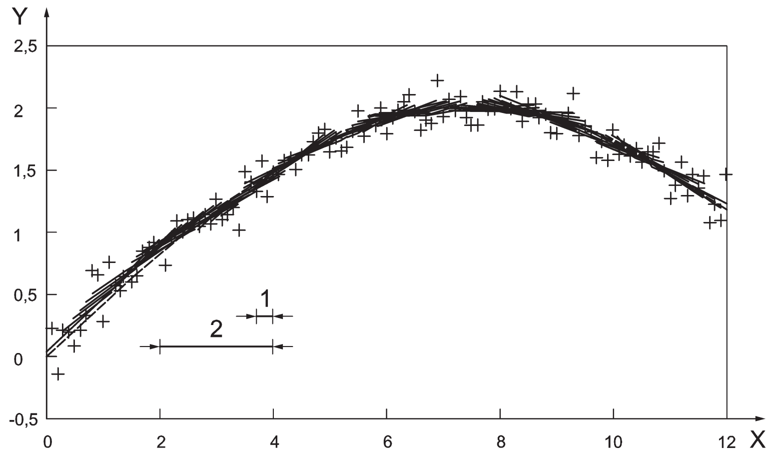

Key

1	spatial sampling interval	X	lateral coordinate (mm)
2	sampling length	Y	f_{det} (µm)
– – – –	real surface after detrending		
+	measurement values after detrending		
———	linear fit		

Figure 4 — Example of the measurement of the one-dimensional slope deviation

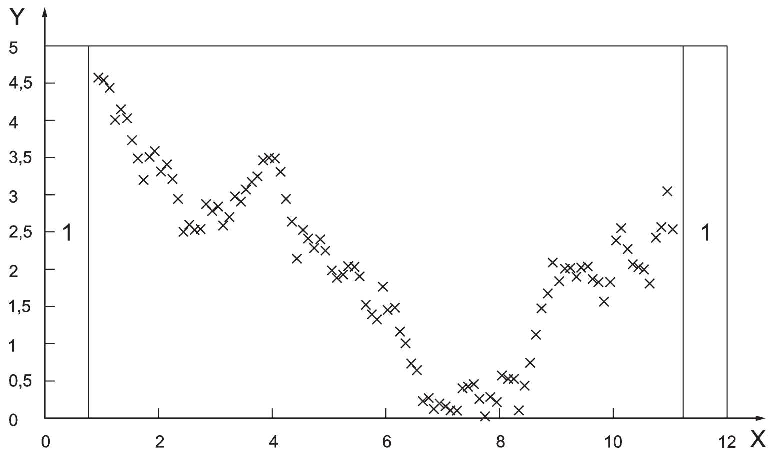

Key

1 non-calculated area

X lateral coordinate (mm)

Y slope deviation (mrad)

Figure 5 — Example of the measurement of the one-dimensional slope deviation

Figure 4 and Figure 5 shows the measurement procedure for the measurement of the one-dimensional slope deviation. For every interval of the sampling length inside the measured cross section, the local slope is calculated by means of a least square fit of a straight line function. The distance between two neighboured intervals for slope calculation equals the spatial sampling interval. The local slope deviation is calculated according to 3.5.2 and is attributed to the centre position of the interval of the sampling length. Hence, for one half of the sampling length on the left and on the right side of the used cross section, no local slope deviation is defined.

For measurement equipment that provides measurement points with a smaller separation than the spatial sampling interval (e.g. scanning instruments), all measurement points within one spatial sampling length shall be used for calculating the least square fit of the straight line function to determine slope deviation for that sampling interval. As above, the distance between two adjacent intervals for calculating the slope deviation equals the spatial sampling interval.

6.2 Two-dimensional measurement of the slope deviation

When using this kind of tolerance definition, the surface data are measured on a two-dimensional grid. This allows the calculation of the slope deviation by means of the gradient of the surface.

Table 2 gives the indication of the tolerance value for ISO 10110-5.

Table 2 — Indication of the tolerance value for two-dimensional measurements

Two-dimensional measurement	Indication	Value	Indication	Value
Slope deviation based on a two-dimensional measurement	$\Delta S_{2\text{-dim}}$	$\max(\xi_{2\text{-dim}})$	$RMS\Delta S_{2\text{-dim}}$	$\text{rms}(\xi_{2\text{-dim}})$

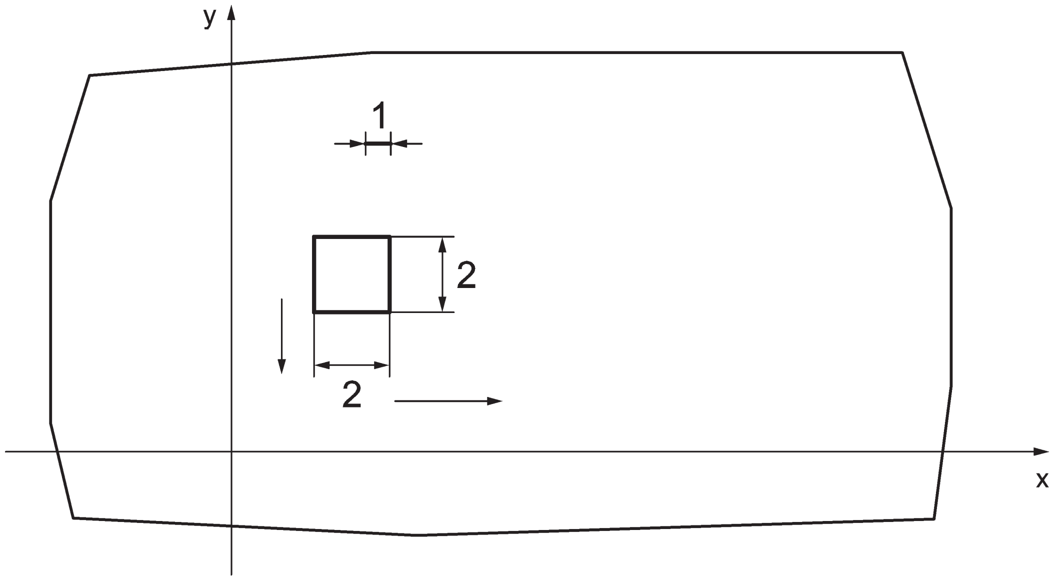

Key

1 spatial sampling interval

2 edge length of sampling area

Figure 6 — Spatial sampling interval and edge length of sampling area for two-dimensional measurement of the slope deviation

Figure 6 indicates the data analysis procedure for the measurement of the two-dimensional slope deviation. For every square with the edge length of the sampling area that is completely contained inside the test area, the local slope is calculated by means of a least square fit of a plane function. The distance between two neighboured squares for slope calculation equals the spatial sampling interval. The local slope deviation is calculated according to 3.5.3 and is attributed to the centre position of the square. Hence, at the border region of the test area, the local slope deviation is not defined, analogous to the one-dimensional case.

For measurement equipment that provides measurement points with a smaller separation than the spatial sampling interval, all measurement points within the square with the edge length of the spatial sampling area shall be used for calculating the least square fit of the plane function to determine slope deviation for that spatial sampling area. As above, the distance between two adjacent squares for calculating the slope deviation is the spatial sampling interval.

Annex A
(normative)

Visual interferogram analysis

A.1 General

A.1.1 General remarks

This Annex is intended as an aid to understanding ISO 10110-5 and ISO 10110-14. It is useful for the interpretation of interferograms (including fringe patterns seen when using test glasses). For surface form measurement, the form deviation is determined by the resulting wavefront deviation as described in the introduction. The guidelines given for the estimation of the amounts of interferograms for the different types of wavefront deformation shall not be regarded as a definition of those wavefront deformation types.

The purpose of this Annex is to demonstrate the visual appearance of interferograms for the different types of wavefront deformation.

This Annex deals exclusively with the following types of wavefront deformation:

— power deviation;

— irregularity;

— rotationally invariant irregularity.

The rms residual wavefront deformation types (defined in 3.3) cannot be determined accurately by visual inspection.

A.2 and A.3 describe the analysis of circular test areas. Special consideration for non-circular test areas is given in A.4.

The analysis of interferograms is described in more detail in many textbooks. See, for example, Reference [5].

A.1.2 Interferometric tilt

Two methods are used for estimating the amounts of power deviation and irregularity, depending on the amount of relative tilt between the test and reference wavefronts. The method without tilt is mainly applied when the wavefront deformation is large. The method employing tilt is generally more accurate.

The relative tilt between the two wavefronts is not a measure of the wavefront deformation.

A.1.3 Determination of the sign of the deformation

In order to determine the sign of the deformation of the wavefront or regions of the wavefront, it is sometimes necessary to slightly shorten or slightly lengthen the test arm of the interferometer, in order to note the behaviour of the interferometric fringes when this is done.

A.2 Estimation of power deviation and irregularity

A.2.1 General

The power deviation can only be determined if the positions of both the object point and the image point are specified. Often, when testing optical elements and systems interferometrically, only one of these two positions is specified and the power deviation cannot be determined; however, the irregularity can still be determined.

NOTE See ISO/TR 14999-1 and ISO/TR 14999-2 for background information on interferometric measurement and illustration of interferometer set-up.

The determination of the power deviation is simplest if the point source of the interferometer is placed at the indicated object point and the mirror that reflects the beam back toward the interferometer is placed concentric with the indicated image point. In the following, it is assumed that this is the case. If this is not the case, then the distances between the indicated and actual object points and the indicated and actual image points is to be taken into account. If dimensional tolerances are associated with the indications of the positions of the object and image points, the source and the reflecting surface may be moved within these tolerances to minimize the power deviation.

Usually, the wavefront deformation is dominated by power deviation and/or by a kind of asymmetry in the power deviation. In the case of asymmetry, cross-sections of the wavefront in different directions show different amounts of power deviation. Other kinds of irregularity are possible; the estimation of their amounts is more difficult. The estimation of the amounts of power deviation and irregularity for the commonly occurring cases is described in A.2.2 and A.2.3, while a more general procedure for unusual types of irregularity is described in A.2.4. The reference given in Reference [5] contains a more thorough discussion of interferogram analysis.

A.2.2 Analysis of interferograms without tilt

In the absence of all other types of wavefront deformation, power deviation causes an interference pattern having concentric, circular fringes. The radii of the fringes increase with the square root of the fringe number, counting from the centre of the interferogram.

If a small amount of asymmetric deformation is present, the circles distort into ellipses, as shown in Figure A.1. If the test wavefront is concave with respect to the reference wavefront, then the fringes will move toward the centre of the fringe pattern when the test arm of the interferometer is shortened. If the reverse is true, then the test wavefront is convex with respect to the reference wavefront.

To estimate the amount of power deviation and irregularity, let m and m' be the numbers of fringe spacings seen in the fringe pattern, counted from the centre to the edge, in the directions that give the largest and smallest numbers of fringes (usually, these two directions are oriented at 90° to one another, but this need not be the case). In the case of elliptical fringes, the power deviation is given by the average of m and m', as given in Formula (A.1):

$$\text{Power deviation (elliptical fringes)} = \frac{m+m'}{2} \quad \text{(A.1)}$$

In the case of elliptical fringes, the wavefront irregularity is equal to the absolute value of the difference of the fringe counts m and m', as given in Formula (A.2):

$$\text{Irregularity (elliptical fringes)} = \left| m - m' \right| \quad \text{(A.2)}$$

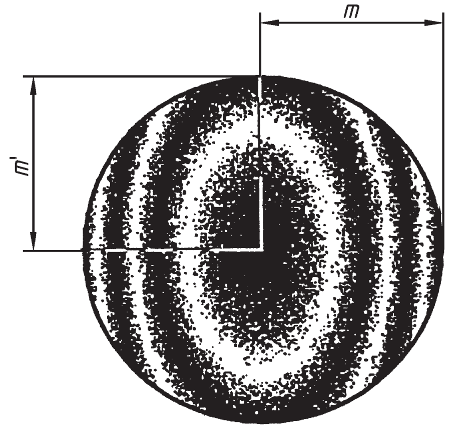

Key

m = 3,0 fringe spacings

m′ = 1,0 fringe spacing

Figure A.1 — Example of an interferogram showing two wavelengths of power deviation and two wavelengths of irregularity (evaluation in Example 1)

EXAMPLE 1 Figure A.1 shows the interferogram of an optical element. The values of m and m' are 3 and 1; therefore, the power deviation [Formula (A.1)] is (3 + 1)/2 = 2 wavelengths, the irregularity [Formula (A.2)] is |3 − 1| = 2 wavelengths.

If a large amount of asymmetric deformation is present, the elliptical fringes may be broken into approximately hyperbolic fringes, as shown in Figure A.2. In this case, when the test wavefront is moved slightly toward the interferometric reference wavefront, some of the fringes will move toward the centre of the fringe pattern and some will move away from the centre.

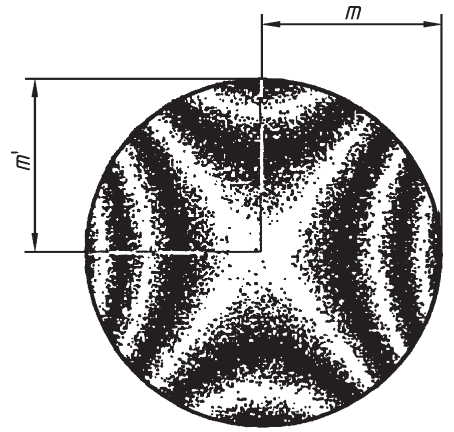

Key

m = 2,5 fringe spacings

m′ = 1,5 fringe spacing

Figure A.2 — Example of an interferogram showing 0,5 wavelengths of power deviation and four wavelengths of irregularity (evaluation in Example 2)

In the case of hyperbolic fringes, the power deviation is equal to half the difference between the numbers of fringe spacings, as given in Formula (A.3):

$$\text{Power deviation (hyperbolic fringes)} = \left| \frac{m - m'}{2} \right| \quad \text{(A.3)}$$

The irregularity in the case of hyperbolic fringes is given by the sum of the numbers of the fringe counts, as shown in Formula (A.4):

$$\text{Irregularity (hyperbolic fringes)} = m + m' \quad \text{(A.4)}$$

EXAMPLE 2 Figure A.2 shows the interferogram of an optical element. The values of m and m' are 2,5 and 1,5 wavelengths, respectively, so the power deviation [Formula (A.3)] is | 2,5 − 1,5 |/2 = 0,5 wavelengths, and the irregularity [Formula (A.4)] is 2,5 + 1,5 = 4 wavelengths.

A.2.3 Analysis of interferograms with tilt

This method requires the fringes to be observed twice, with the tilt between the test and reference wavefronts adjusted so that the fringes are oriented in two different directions.

When the reference surface is tilted with respect to the test surface, the fringes appear as in Figure A.3. If only power deviation is present, then the fringes appear as parts of concentric circles, with the radii of the fringes increasing with the square root of the fringe number, counting from the apparent centre of the interferogram. If other wavefront deformation types are also present, the fringes are not parts of concentric circles.

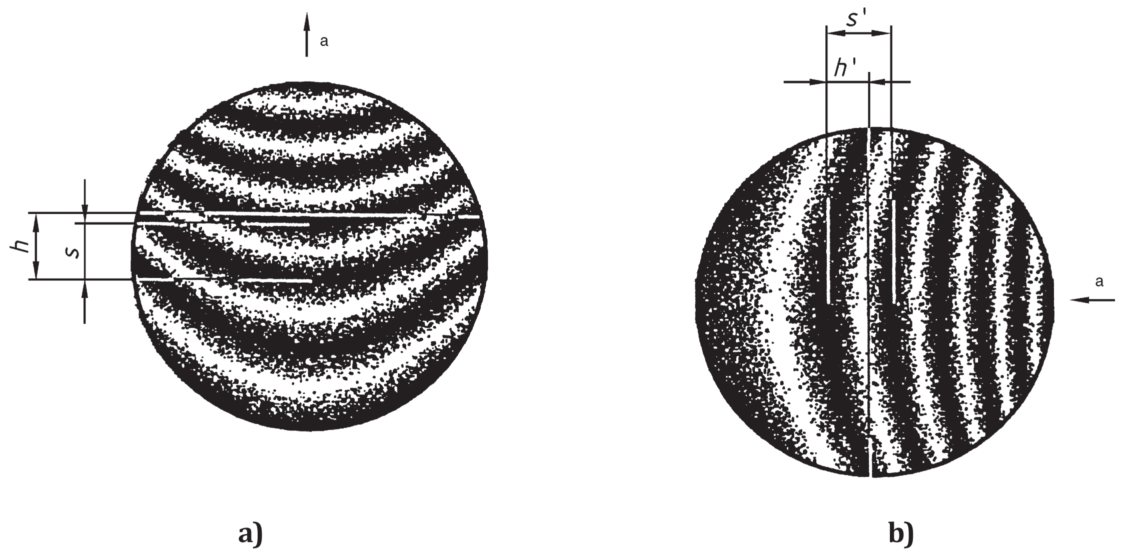

Key

m = h/s

m' = h'/s'

a Motion: the arrows indicate the direction of motion of fringes when the test arm is shortened.

Figure A.3 — Example showing interferograms with 0,3 wavelengths of power deviation and 1,8 wavelengths of irregularity, with the interferometric tilt oriented in two directions (evaluation in Example 3)

To estimate the power deviation and the irregularity, the curvature of the test wavefront in the cross-section parallel to the fringes is estimated for the two directions of tilt that give the maximum and minimum amounts of curvature [see Figure A.3 a) and Figure A.3 b)]. In each case, the number of fringe spacings, *m*, is equal to the curvature, *h*, of the fringe closest to the centre of the interferogram, divided by the spacing, *s*, of the fringes, which is also measured as close as possible to the centre of the test area.

In addition, it is necessary to note (for both directions of the tilt) the direction of motion of the fringes when the test arm of the interferometer is shortened (the surface under test is moved slightly towards the reference surface).

If the fringes for both directions of tilt move toward the apparent centre of curvature of the fringes or if the fringes for both directions of tilt move away from the apparent centre, then the power deviation exceeds the irregularity and Formula (A.1) and Formula (A.2) are used to estimate the power deviation and the irregularity, respectively.

If one set of fringes moves towards its apparent centre and the other fringe pattern moves away from its apparent centre when the test arm is shortened, then the irregularity exceeds the power deviation and Formula (A.3) and Formula (A.4) are used to estimate the amounts of power deviation and irregularity, respectively.

EXAMPLE 3 Figure A.3 shows interferograms of an optical element tested with tilt. In Figure A.3 a), the fringes move towards the apparent centre when the test arm is shortened while in Figure A.3 b), the fringes move away from the apparent centre, so Formula (A.3) and Formula (A.4) apply. In Figure A.3 a), the curvature, *h*, is approximately 1,2× the fringe spacing, *s*, so $m = 1{,}2$. In Figure A.3 b), the curvature, h', is 60 % the fringe spacing, s', so $m' = 0{,}6$. The immediate result of Formula (A.3) is 0,3 wavelengths for the power deviation. Similarly, Formula (A.4) yields a value of 1,8 wavelengths for the irregularity.

A.2.4 Unusual forms of irregularity

It is possible that the wavefront deformation be at maximum at some point inside the test area, rather than at the edge. When testing wavefronts with no tilt between the test and reference wavefronts, this leads to closed fringes which might not be concentric with the centre of the test area, as shown in Figure A.4. In such cases, it is necessary to note which fringes move away from the centre and which move toward the centre when the test arm of the interferometer is shortened. Those that move toward the centre may be regarded as “positive” and the others as “negative”.

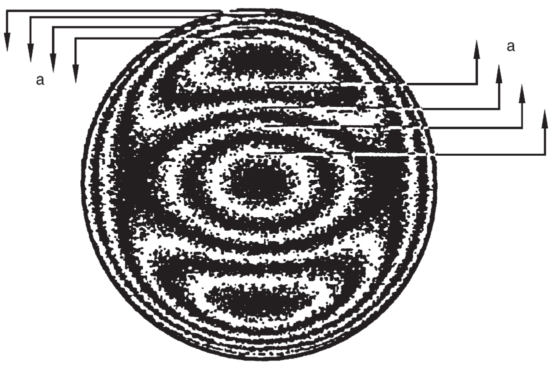

a Motion.

Figure A.4 — Example of an unusual interferogram, showing the direction of motion of the fringes when the test arm of the interferometer is shortened (evaluation in Example 4)

EXAMPLE 4 The power deviation is determined according to Formula (A.1), where *m* and m' represent the cumulative numbers of fringes measured in two representative directions. In the vertical cross-section of Figure A.4, there are four fringe spacings in the negative direction, followed by four fringe spacings in the positive direction, giving a value of zero for *m*. In the horizontal direction, there are two negative and two positive fringes, again giving $m' = 0$. According to Formula (A.1), the power deviation is $(0 + 0)/2 = 0$.

The irregularity is determined by finding the highest and lowest departures from the theoretical expected fringe pattern, which is that the fringes are concentric circles with radii increasing as the square root of the fringe number. The irregularity is the sum of the absolute values of the highest and lowest departures from the pattern. For the pattern of Figure A.4, the power deviation is zero, so the theoretical expected fringe pattern has no fringes. The lowest departure from this is −4 fringe spacings (at the centres of the two outer oval patterns) and the highest departure from this is zero. Therefore, the irregularity is |0| + |−4| = 4 fringes.

A.3 Estimation of rotationally invariant irregularity

The estimation of this deviation by visual methods is difficult if large amounts of other types of wavefront deformation are present. For this reason, digital methods of interferogram analysis are preferred.

If no tilt is present between the test wavefront and the reference wavefront, the fringes appear as concentric circles but their radii do not increase with the square root of the fringe number as would be the case with power deviation. Visual observation of this property is difficult and becomes inaccurate for small deviations. Therefore, the assessment of this type of wavefront deformation is practical only in the presence of tilt.

In the presence of tilt, the fringes are W-shaped or M-shaped, depending on the direction of the tilt. In the absence of power deviation, the two ends and the centre of the fringe nearest the centre of the fringe pattern can be joined by a straight line. In this case, the irregularity is represented by the deviation of the fringes from straightness. If power deviation is present in the wavefront, the fringes are curved (as shown in Figure A.5) and the irregularity is estimated by the deviation of the fringe nearest the centre from a circular arc joining the two ends and the centre of the fringe.

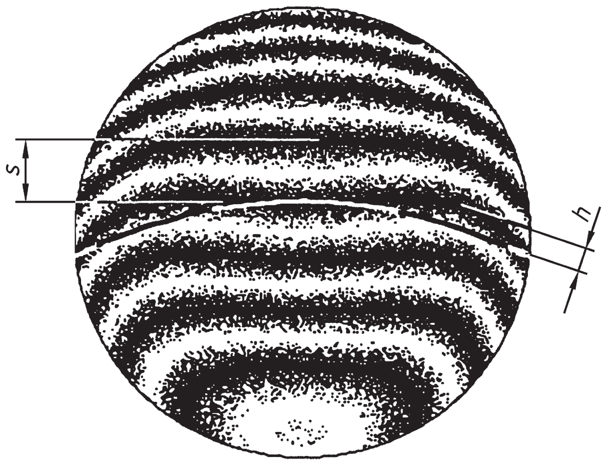

Figure A.5 — Example of an interferogram showing 0,3 wavelengths of rotationally invariant irregularity (evaluation in Example 5)

The irregularity is equal to the maximum deviation, h, of the fringe from a circular arc, divided by the fringe spacing, s. The deviation, h, is measured perpendicular to the circular arc at the point of maximum departure.

The rotationally invariant irregularity is given by Formula (A.5):

$$\text{Rotationally invariant irregularity} = \frac{h}{s} \quad (A.5)$$

EXAMPLE 5 In Figure A.5, the deviation, h, of the central fringe from a circular arc is 30 % of the fringe spacing, s, so the rotationally invariant irregularity is 0,3 fringe spacings [the result of Formula (A.5)].

The degree to which the wavefront deformation is rotationally invariant is observed by repeating the above test with the tilt adjusted so that the fringes are oriented in another direction. The wavefront deformation is rotationally invariant if the appearance of the fringes is the same for all orientations of the fringes. The rotationally invariant irregularity is that part of the deformation which remains the same for all orientations of the fringes.

A.4 Non-circular test areas

According to the definition, the power deviation (see 3.3.1) is based on the spherical wavefront that best approximates the test wavefront. When using visual analysis methods, the wavefront spherical approximation (see 3.2.6) can be chosen so that the wavefront irregularity (see 3.2.8) is evenly distributed around the boundary of the test area. This requires that power deviation and irregularity be evaluated by a method similar to that described in A.2, except that the calculations shall take into account the dimensions of the test area in the two cross-sections in which m and m' are measured.

This method is reasonably accurate for simple forms of wavefront deformation (i.e. those which are second-order in x and y); for an accurate evaluation of more complex forms, digital methods are necessary.

For non-circular test areas, the “centre” of the test area refers to its centroid (“centre-of-gravity”) and its “radius” is equal to the distance from the centre to the most distant point in the test area.

The cross-sectional curvatures m and m' are determined in the same way as in A.2, using the description of the case with or without tilt, as appropriate. The directions along which m and m' are determined are given by the symmetry of the wavefront deformation; these directions are not necessarily related to the shape of the test area.

Let m and m' be the cross-sectional curvatures in the two directions of symmetry from the centre to the edge of the test area, as shown in Figure A.6. Let a be the distance from the centre to the edge of the test area in the direction along which the curvature, m, is measured. Similarly, let b be the distance along which the curvature m' is measured. Let R be the radius of the test area, as defined above.

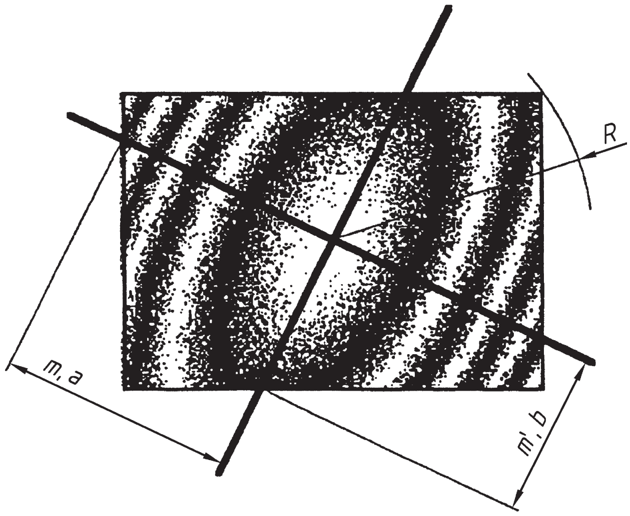

Key

R = 36 mm

m = 3,6 fringe spacings

a = 33 mm

m' = 0,4 fringe spacings

b = 23 mm

Figure A.6 — Example of an interferogram with a non-circular test area, showing 3,2 wavelengths of power deviation and 2,2 wavelengths of irregularity (evaluation in Example 6)

In the case of elliptical fringes and a non-circular test area, the power deviation is determined by Formula (A.6):

$$\text{Power deviation (elliptical fringes)} = \frac{R^2\left(m+m'\right)}{a^2+b^2} \tag{A.6}$$

In the case of elliptical fringes and a non-circular test area, the irregularity is determined by Formula (A.7):

$$\text{Irregularity (elliptical fringes)} = \left|\frac{2R^2\left(a^2m'-b^2m\right)}{a^2\left(a^2+b^2\right)}\right| \tag{A.7}$$

EXAMPLE 6 In Figure A.6, the values of m and m' are 3,6 and 0,4 wavelengths, measured over distances of 33 mm and 23 mm, respectively. The radius of the test area is 36 mm. The results of Formula (A.6) and Formula (A.7) are 3,2 wavelengths and 2,16 wavelengths, respectively. Thus, the power deviation is 3,2 wavelengths and the irregularity is 2,16 wavelengths.

In the case of hyperbolic fringes, the power deviation is found by Formula (A.8):

$$\text{Power deviation (hyperbolic fringes)} = \left|\frac{R^2\left(m-m'\right)}{a^2+b^2}\right| \tag{A.8}$$

In the case of hyperbolic fringes, the irregularity is found by Formula (A.9):

$$\text{Irregularity (hyperbolic fringes)} = \frac{2R^2\left(a^2m'+b^2m\right)}{a^2\left(a^2+b^2\right)} \tag{A.9}$$

If there is tilt between the interferometric reference wavefront and the wavefront under test, then it is necessary to note (for both directions of the tilt) the direction of motion of the fringes when the test arm of the interferometer is shortened.

If the fringes in both cases move towards the apparent centre of the fringe pattern or if the fringes in both cases move away from the apparent centre of the fringe pattern, then the power deviation exceeds the irregularity and Formula (A.6) and Formula (A.7) shall be used to estimate the power deviation and the irregularity.

If one set of fringes moves towards its apparent centre and the other fringe pattern moves away from its apparent centre, then the irregularity exceeds the power deviation and Formula (A.8) and Formula (A.9) shall be used to estimate the amounts of power deviation and irregularity.

A.5 Target aberrations

The visual analysis of interferograms when target aberrations are specified is difficult and not recommended. In principle, it is possible to draw or otherwise generate the interference pattern corresponding to the target aberrations and examine the difference between this and the actual interferogram; however, the visual appearance of the actual interferogram depends on the amount and orientation of tilt present. Similarly, the exact choice of the radius of the reference sphere, which often has a generous tolerance, influences the visual appearance of the interference pattern. For these reasons, the precise generation of the theoretical interference pattern with which the actual interferogram should be compared to is generally not possible, in which case, an accurate evaluation can be obtained only through the use of digital analysis techniques.

Annex B
(normative)

Zernike polynomials

A detailed discussion of the use of the Zernike polynomials is given in ISO/TR 14999-2.

For the Zernike coefficients, different single number ordering systems are in use. Commonly, a system is used where the numbering starts with 0 denoting the piston term. However, ISO/TR 14999-2 starts with 0 denoting a tilt term. Without explicit definition, it is not obvious which system is used.

Therefore, this Annex defines the system Z(n, m) as the ordering system, see Table B.1.

Referencing to individual Zernike coefficients:

For referencing to individual Zernike coefficients, use Z(n, m). For instance, Z(4,0) refers to the spherical aberration of the first order, Z(3,1) refers to the coma of the first order in the x direction.

Referencing to a group of Zernike coefficients:

For referencing to a group of Zernike coefficients, use the letter N in parentheses. For instance, Z(N = 2), refers to the Zernike coefficients of the group N = 2, Z(N = 2,4,6) refers to the Zernike coefficients of the groups N = 2, 4, 6.

Referencing to a group of Zernike coefficients and to individual Zernike coefficients:

For referencing to a combination of a group of Zernike coefficients and individual coefficients, use the group reference and the individual reference separated by one or more commas. For instance, Z(N = 4),Z(6,0) refers to the Zernike coefficients of the group N = 4 and the Zernike coefficient Z(6, 0).

Table B.1 — Circular — Zernike (“C-P-P”)

Orthogonal on the circle (extendible to the ellipses)		
Polar variables: (r, θ)		
Expressed in polar coordinates: $\Sigma\ \{P_n(r)\cos(m\theta)\}$ for m > 0 **or** $\Sigma\ \{P_n(r)\sin(-m\theta)\}$ for m < 0 ; $N = n + \|m\|;\ n \geq \|m\|$		
N	n, m	Formula
0	0, 0	1
2	1, 1	$r\cos\theta$
:	1, −1	$r\sin\theta$
2	2, 0	$2r^2 - 1$
4	2, 2	$r^2\cos2\theta$
:	2, −2	$r^2\sin2\theta$
:	3, 1	$(3r^2 - 2)\ r\cos\theta$
:	3, −1	$(3r^2 - 2)\ r\sin\theta$
4	4, 0	$6r^4 - 6r^2 + 1$
6	3, 3	$r^3\cos3\theta$
:	3, −3	$r^3\sin3\theta$
:	4, 2	$(4r^2 - 3)\ r^2\cos2\theta$
:	4, −2	$(4r^2 - 3)\ r^2\sin2\theta$
:	5, 1	$(10r^4 - 12r^2 + 3)\ r\cos\theta$

Table B.1 *(continued)*

Orthogonal on the circle (extendible to the ellipses) Polar variables: (r, θ) Expressed in polar coordinates: $\Sigma \{P_n(r) \cos(m\theta)\}$ for m > 0 or $\Sigma \{P_n(r) \sin(-m\theta)\}$ for m < 0 ; $N = n + \|m\|$; $n \geq \|m\|$		
N	n, m	Formula
:	5, –1	$(10r^4 - 12r^2 + 3)\ r\sin\theta$
6	6, 0	$20r^6 - 30r^4 + 12r^2 - 1$
8	4, 4	$r^4\cos4\theta$
:	4, –4	$r^4\sin4\theta$
:	5, 3	$(5r^2 - 4)\ r^3\cos3\theta$
:	5, –3	$(5r^2 - 4)\ r^3\sin3\theta$
:	6, 2	$(15r^4 - 20r^2 + 6)\ r^2\cos2\theta$
:	6, –2	$(15r^4 - 20r^2 + 6)\ r^2\sin2\theta$
:	7, 1	$(35r^6 - 60r^4 + 30r^2 - 4)\ r\cos\theta$
:	7, –1	$(35r^6 - 60r^4 + 30r^2 - 4)\ r\sin\theta$
8	8, 0	$70r^8 - 140r^6 + 90r^4 - 20r^2 + 1$
10	5, 5	$r^5\cos5\theta$
:	5, –5	$r^5\sin5\theta$
:	6, 4	$(6r^2 - 5)\ r^4\cos4\theta$
:	6, –4	$(6r^2 - 5)\ r^4\sin4\theta$
:	7, 3	$(21r^4 - 30r^2 + 10)\ r^3\cos3\theta$
:	7, –3	$(21r^4 - 30r^2 + 10)\ r^3\sin3\theta$
:	8, 2	$(56r^6 - 105r^4 + 60r^2 - 10)\ r^2\cos2\theta$
:	8, –2	$(56r^6 - 105r^4 + 60r^2 - 10)\ r^2\sin2\theta$
:	9, 1	$(126r^8 - 280r^6 + 210r^4 - 60r^2 + 5)\ r\cos\theta$
:	9, –1	$(126r^8 - 280r^6 + 210r^4 - 60r^2 + 5)\ r\sin\theta$
10	10, 0	$252r^{10} - 630r^8 + 560r^6 - 210r^4 + 30r^2 - 1$
12	6, 6	$r^6\cos6\theta$
:	6, –6	$r^6\sin6\theta$
:	7, 5	$(7r^2 - 6)\ r^5\cos5\theta$
:	7, –5	$(7r^2 - 6)\ r^5\sin5\theta$
:	8, 4	$(28r^4 - 42r^2 + 15)\ r^4\cos4\theta$
:	8,- 4	$(28r^4 - 42r^2 + 15)\ r^4\sin4\theta$
:	9, 3	$(84r^6 - 168r^4 + 105r^2 - 20)\ r^3\cos3\theta$
:	9, –3	$(84r^6 - 168r^4 + 105r^2 - 20)\ r^3\sin3\theta$
:	10, 2	$(210r^8 - 504r^6 + 420r^4 - 140r^2 + 15)\ r^2\cos2\theta$
:	10, –2	$(210r^8 - 504r^6 + 420r^4 - 140r^2 + 15)\ r^2\sin2\theta$
:	11, 1	$(462r^{10} - 1\,260r^8 + 1\,260r^6 - 560r^4 + 105r^2 - 6)\ r\cos\theta$
:	11, –1	$(462r^{10} - 1\,260r^8 + 1\,260r^6 - 560r^4 + 105r^2 - 6)\ r\sin\theta$
12	12, 0	$924r^{12} - 2\,772r^{10} + 3\,150r^8 - 1\,680r^6 + 420r^4 - 42r^2 + 1$

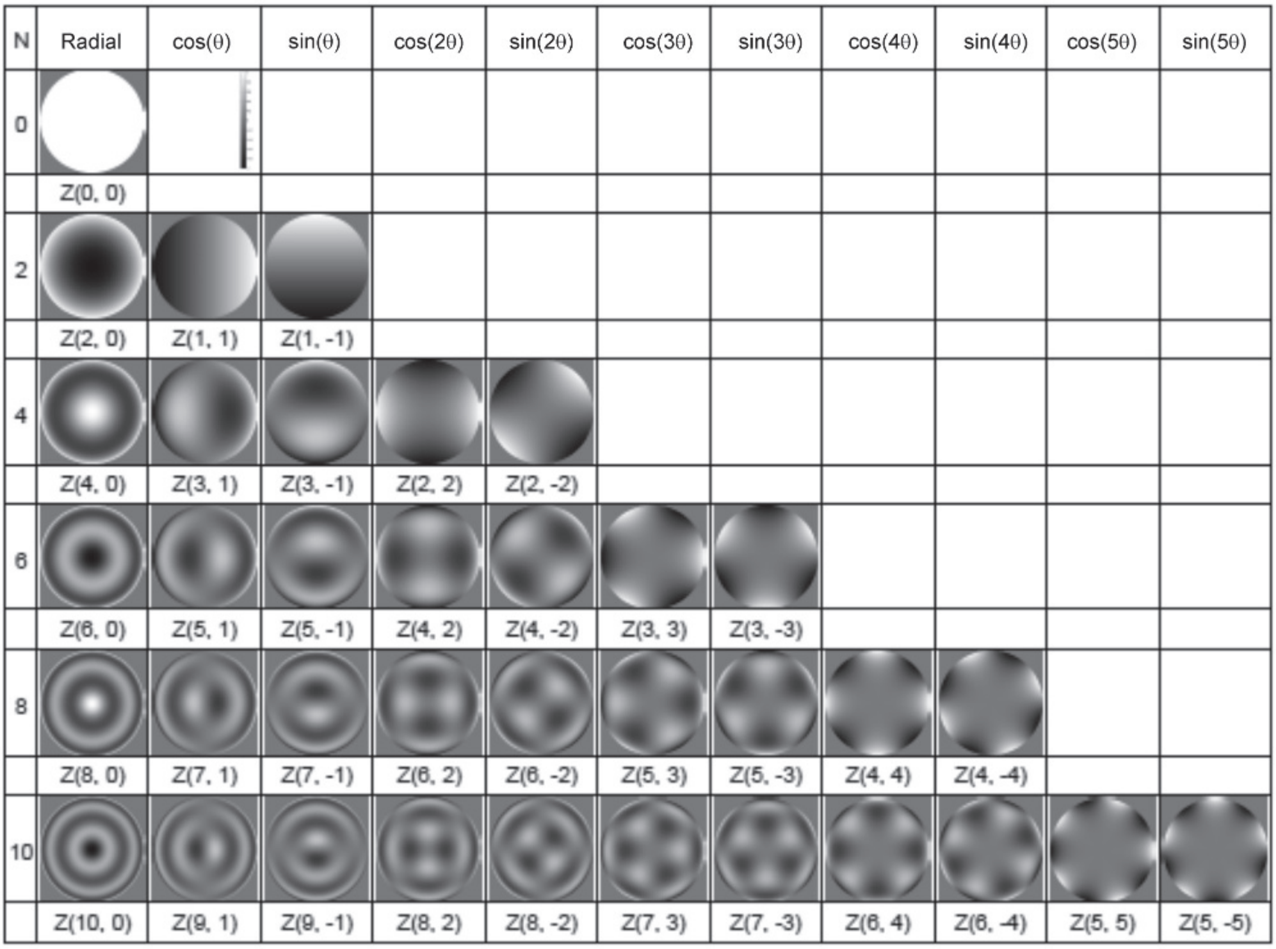

Figure B.1 — Example of visualization of Zernike orthogonal set Z($N \leq 10$)

Bibliography

[1] ISO 4287, *Geometrical Product Specifications (GPS) — Surface texture: Profile method — Terms, definitions and surface texture parameters*

[2] ISO 25178 (all parts), *Geometrical product specification (GPS) — Surface texture: Areal*

[3] ISO/TR 14999-1, *Optics and photonics — Interferometric measurement of optical elements and optical systems — Part 1: Terms, definitions and fundamental relationships*

[4] Evans C.J. Opt. Eng. 2009, **48** p. 043605

[5] Malacara D. ed. Optical shop testing. Wiley, New York, Third Edition, 2007

ICS 37.020

Price based on 27 pages

This page deliberately left blank

British Standards Institution (BSI)

BSI is the national body responsible for preparing British Standards and other standards-related publications, information and services.

BSI is incorporated by Royal Charter. British Standards and other standardization products are published by BSI Standards Limited.

About us

We bring together business, industry, government, consumers, innovators and others to shape their combined experience and expertise into standards -based solutions.

The knowledge embodied in our standards has been carefully assembled in a dependable format and refined through our open consultation process. Organizations of all sizes and across all sectors choose standards to help them achieve their goals.

Information on standards

We can provide you with the knowledge that your organization needs to succeed. Find out more about British Standards by visiting our website at bsigroup.com/standards or contacting our Customer Services team or Knowledge Centre.

Buying standards

You can buy and download PDF versions of BSI publications, including British and adopted European and international standards, through our website at bsigroup.com/shop, where hard copies can also be purchased.

If you need international and foreign standards from other Standards Development Organizations, hard copies can be ordered from our Customer Services team.

Subscriptions

Our range of subscription services are designed to make using standards easier for you. For further information on our subscription products go to bsigroup.com/subscriptions.

With **British Standards Online (BSOL)** you'll have instant access to over 55,000 British and adopted European and international standards from your desktop. It's available 24/7 and is refreshed daily so you'll always be up to date.

You can keep in touch with standards developments and receive substantial discounts on the purchase price of standards, both in single copy and subscription format, by becoming a **BSI Subscribing Member**.

PLUS is an updating service exclusive to BSI Subscribing Members. You will automatically receive the latest hard copy of your standards when they're revised or replaced.

To find out more about becoming a BSI Subscribing Member and the benefits of membership, please visit bsigroup.com/shop.

With a **Multi-User Network Licence (MUNL)** you are able to host standards publications on your intranet. Licences can cover as few or as many users as you wish. With updates supplied as soon as they're available, you can be sure your documentation is current. For further information, email bsmusales@bsigroup.com.

Revisions

Our British Standards and other publications are updated by amendment or revision.

We continually improve the quality of our products and services to benefit your business. If you find an inaccuracy or ambiguity within a British Standard or other BSI publication please inform the Knowledge Centre.

Copyright

Useful Contacts:

Customer Services
Tel: +44 845 086 9001
Email (orders): orders@bsigroup.com
Email (enquiries): cservices@bsigroup.com

Subscriptions
Tel: +44 845 086 9001
Email: subscriptions@bsigroup.com

Knowledge Centre
Tel: +44 20 8996 7004
Email: knowledgecentre@bsigroup.com

Copyright & Licensing
Tel: +44 20 8996 7070
Email: copyright@bsigroup.com

BSI Group Headquarters

389 Chiswick High Road London W4 4AL UK

bsi.

...making excellence a habit.™